DOI: 10.24850/j-tyca-2026-01-03

Articles

Removal of copper salts by sodalite coated with layered double hydroxides

Remoción de sales de cobre por sodalitas recubiertas con hidróxidos doble laminares

Andrea P. Aparicio[1], ORCID: https://orcid.org/0000-0002-2361-3112

José H. Quintana-Mendoza[2], ORCID: https://orcid.org/0000-0002-7107-5830

J. A. Henao[3], ORCID: https://orcid.org/0000-0002-2887-1532

[1]Grupo de Investigación GIAU-ECBTI, Universidad Nacional Abierta y a Distancia, Bucaramanga-Santander, Colombia, Andrea_24sanchez@hotmail.com

[2]Grupo de investigación CIDAGRO-ECAPMA, Universidad Nacional Abierta y a Distancia, Bucaramanga-Colombia, jhquintanam@gmail.com

[3]Grupo de Investigación GIQUE, Universidad Industrial de Santander, Bucaramanga-Santander, Colombia, jahenao@uis.edu.co

Corresponding author: José H. Quintana Mendoza, jhquintanam@gmail.com

Tecnología y Ciencias del Agua

OPEN ACCESS

Check for updates

Abstract

Sodalite type zeolite from silicon and aluminum post consume was coated with layered double hydroxide (molar relationship Mg^{2+} / Al^{3+} = 2) by co-precipitation to low saturated method. The structural, morphological and textural properties for the zeolite, LDH and coated material were characterized by the powder X-ray diffraction (XRD), scanning electron microscopy (SEM), Nuclear Magnetic Resonance spectroscopy (NMR) 27Al and textural measurements. The solids obtained were used by removal Cu^{2+}, Cl^{-}, NO_3^{-} and SO_4^{2-} from $Cu(NO_3)_2$, $CuCl_2$ and $CuSO_4$ solutions. Removal capacity was studied by X-ray Fluorescence spectrometry (XFR) (for Cu, Cl and S) and UV-vis spectroscopy (NO_3^{-}), the results were showed the sodalite coated with LDH retained simultaneous uptake cations and anions Cu^{2+} (9.26 mmol*g^{-1}), Cl^{-} (9.34 mmol*g^{-1}), SO_4^{2-} (8.82 mmol*g^{-1}) and NO_3^{-} (14.41 mmol*g^{-1}). These results show zeolites coated with LDH can using how removal harmful cations and anions and catalysts.

Keywords: Cations and anions adsorption, LDH, XRD, SEM, NMR, zeolite, sodalite type, water remediation.

Resumen

Se sintetizaron zeolitas tipo sodalita a partir de silicio y aluminio posconsumo, las cuales se recubrieron con el hidróxido doble laminar (HDL) con una relación molar Mg^{2+} / Al^{3+} = 2, que se formaron por el método de coprecipitación a baja saturación. Las propiedades estructurales, morfológicas y texturales de la zeolita, el HDL y el material recubierto se determinaron mediante difracción de rayos X de muestras policristalinas (XRD), microscopía electrónica de barrido (SEM),

espectroscopía de resonancia magnética nuclear 27Al (RMN) y medidas texturales. Los sólidos obtenidos se utilizaron para la eliminación de Cu^{2+}, Cl^-, NO_3^- y SO_4^{2-} desde soluciones acuosas de $Cu(NO_3)_2$, $CuCl_2$ y $CuSO_4$, estudiando la capacidad de remoción por espectrometría de fluorescencia de rayos X (XFR) para Cu^{2+}, Cl^- y SO_4^{2-}, y espectroscopía UV-Vis para el NO_3^-. Los resultados mostraron que la zeolita tipo sodalita recubierta con HDL fue capaz de hacer la captación simultánea de cationes y aniones como el Cu^{2+} en 9.26 mmol*g^{-1}, Cl^- en 9.34 mmol*g^{-1}, SO_4^{2-} en 8.82 mmol*g^{-1} y NO_3^- en 14.41 mmol*g^{-1}. Estos resultados muestran que las zeolitas recubiertas con HDL se pueden usar para retener cationes y aniones dañinos para el medio ambiente, y representan una oportunidad para diseñar catalizadores

Palabras clave: adsorción de aniones y cationes, HDL, XRD, SEM, RMN, zeolita, tipo sodalita, remediación del agua.

Received: 14/10/2024

Accepted: 07/04/2025

Available ahead of print: 29/04/2025

Version of record: 01/01/2026

Introduction

LDHs are a group of clays or hydrotalcite-like compounds with a CdI_2 -type structure, containing M^{2+} and M^{3+} cations within hydroxide layers with the general composition ($M^{2+}_{(1-x)}$ $M^{3+}_x(OH)_2$), resulting in a residual positive charge. This charge is compensated in the interlayer space by anions ($Y_x/$□), where 'Y' is the interlayer anion, 'n' is the charge of the

interlayer anion, and x is the molar ratio (M^{3+} / (M^{2+} + M^{3+}) (Theiss, Couperthwaite, Ayoko, & Frost, 2014; Chung *et al*., 2020). These anions are exchangeable depending on synthesis conditions, which makes LDHs useful for various applications such as the intercalation of biomolecules and surfactants (Kumari *et al*., 2023), controlled drug release (Guilherme, Cunha, De Paula, De Araujo, & Constantino, 2022), photocatalysts for H_2 (g)/O_2 (g) generation (Yang *et al*., 2021), oxidation and catalysis of contaminants in wastewater (Xie *et al*., 2021), and internal reactions for biomass transformation (Li *et al.*, 2024).

Zeolites are microporous crystalline solids with molecular-scale dimensions that accommodate exchangeable cations. Their three-dimensional framework is composed of tetrahedral units consisting of four oxygen atoms surrounding a T cation (T = Si, Al, B, Be, Co, Ga, Ge, Fe, P, Zn), interconnected through oxygen atoms to form tectosilicates. These frameworks are capable of cation exchange and can selectively host organic molecules, such as leachates and/or nutrients, making them useful in agriculture and environmental protection (Cataldo *et al*., 2021; Szerement, Szatanik-Kloc, Jarosz, Bajda, & Mierzwa-Hersztek, 2021; Yuan, Han, Deng, Zhou, & Zhou, 2024). Zeolites can also be used to deposit chemical species such as rhodium, calcium, chlorine, copper, and chromium on their surfaces or within their cavities for applications in fine organic synthesis and/or high-efficiency catalytic production (López, Toro, Romero-Bohórquez, Quintana, & Henao, 2020; Weitkamp, 2020; Zhang *et al*., 2023; Liu *et al*., 2024).

According to the strong anion and cation removal abilities known in LDHs and zeolites, the aim is to develop a material that integrates both tectosilicate and layered double hydroxide (LDH) structures. A first step in this area was the incorporation of Mg-Al LDHs into an LTA-type zeolite

(Yamada *et al*., 2006) and their application for the removal of copper anions and cations from wastewater at low concentrations (Bezerra, Bieseki, Da Silva, & Pergher, 2019). For the removal of Cr^{6+}, hydrotalcites, LDH-Cl, and natural zeolites combined with LDHs have been used ((Wang, Zhou, Achari, Yu, & Cai, 2014; Yue, Liu, Chen, & Lin, 2017; Zhang *et al*., 2019a; Zhang *et al*., 2019b). In the case of Cd^{2+} retention (1,428.57 $mg \cdot kg^{-1}$), zeolites combined with Zn-, Mg-, and Fe-based LDHs have been employed, and similar systems have also been used for nitrogen and phosphorus fixation (Yuan *et al*., 2018; Zhang *et al*., 2019a; Ji *et al*., 2020). The present study seeks to use a more basic zeolite, such as sodalite—with smaller cages and increased surface area—coated with Mg-Al LDH in order to develop a material with high capacity for the removal of anions and cations from copper-containing solutions. This could facilitate the development of heterogeneous catalysts for polymerization processes (Hong *et al*., 2004) or for water electrolysis (Lee, Wu, & Sun, 2020).

Materials and methods

Materials

Sodium silicate and aluminate solutions were obtained from waste silica sourced from conventional chromatography columns and post-consumer aluminum from food packaging. The following reagents were used: NaOH (MERCK), $MgCl_2 \cdot 6H_2O$ (MERCK), $AlCl_3 \cdot 6H_2O$ (MERCK), Na_2CO_3 (MERCK), $Cu(NO_3)_2$ (MERCK), $CuCl_2$ (MERCK), and $CuSO_4$ (MERCK). All synthesized solids were washed with deionized water and dried at 298 K. Each solid was synthesized in triplicate.

Synthesis of precursors

For the treatment of post-consumer silicon, the purification process reported by Teixeira, Mathias and Canela (2003); was applied. The purified silicon was then mixed stoichiometrically with 3 M NaOH at 363 K under reflux for 2 hours. After the reaction, the mixture was filtered, and the sodium silicate solution (filtrate) was characterized by atomic absorption spectroscopy using a THERMO ELECTRON instrument equipped with a silicon hollow cathode lamp. A concentration of 30,000 mg/L of silicon was obtained. The solution was then concentrated by evaporation at 350 K until reaching a final silicon concentration of 60,000 mg/L.

For the sodium aluminate solution, aluminum foil was washed with water and dried at 298 K. The aluminum was then treated stoichiometrically with 3 M NaOH until hydrogen gas evolution ceased, following the procedure described by Quintana, Aparicio, Parra, Henao and Ríos (2014). The resulting filtrate was characterized by atomic absorption spectroscopy using a THERMO ELECTRON instrument with an aluminum hollow cathode lamp, yielding a concentration of 100,000 mg/L of aluminum.

Synthesis of the zeolite

A solution A was prepared by mixing 15.5 ml of sodium aluminate with 3.1 g of NaOH, and solution B was prepared by mixing 26.8 ml of sodium silicate. The two solutions were then mixed drop by drop in a 65 ml Teflon reactor, ensuring that the reactor was 65 % full. During the mixing, the reaction was kept under constant agitation at 250 rpm. After the addition

was complete, the reactor was sealed and heated at 363 K for 32 hours. At the end of this period, the mixture was filtered, the solid was washed, and then dried at 50 °C for 12 hours. The resulting material was designated SOD1.

To reduce the crystal size of the previously synthesized material, 1.000 g of SOD1 was mixed with 82.5 mL of 0.01 M aluminum chloride solution. The mixture was then subjected to reflux at 750 rpm for 2 hours. After the process, the mixture was filtered, washed with distilled water until neutral pH was reached, and dried at 50 °C for 12 hours to obtain the solid SOD2.

Synthesis of the layered double hydroxide

The HDL was synthesized using a low saturation coprecipitation method. Solutions of hexahydrate aluminum chloride and hexahydrate magnesium chloride were mixed with a molar ratio of Mg/Al equal to 2. Starting with 1.0000 g of aluminum salt, it was combined with magnesium salt and diluted to 25 ml. As the precipitating solution, 0.2000 g of sodium carbonate was dissolved in 25 ml of a 3 M sodium hydroxide solution. The pH was adjusted to 9, and the mixture was stirred for 30 minutes. The crude reaction mixture was then aged at 363 K for 9 hours. The solid was filtered, dried at 50 °C for 12 hours, and was manned as HDL2.

Synthesis of Zeolites Coated with Layered Double Hydroxides

Starting with 1.0000 g of SOD2, it was treated at 573 K for 1 hour under a constant flow of N2(g). Then, without removing the inert flow, the solid

was cooled to 273 K. Subsequently, 25 ml of a solution containing aluminum and magnesium cations in a molar ratio of 2 (prepared from $MgCl_2 \cdot 6H_2O$ and 1.0000 g of $Al(NO_3)_3 \cdot 6H_2O$) was added. Next, 25 ml of 3M NaOH, prepared with decarbonated water under argon, was added to the mixture. Finally, the reaction was treated at 362 K for 9 hours under magnetic stirring at 750 rpm. The filtered solid was washed with distilled water until neutral pH was reached and then dried at 50 °C. The resulting material was designated as SOD2-HDL2.

Ion exchange study

For ion fixation, 0.1000 g of SOD1 was mixed with 20 mL of 0.02 M $Cu(NO_3)_2$ and stirred at 500 rpm for 30 minutes. After the designated time, the mixture was filtered, and the filtrate was characterized. The procedure was repeated for the materials HDL2, SOD2, and SOD2-HDL2, with each material, but replacing the copper solution with $CuCl_2$ and then $CuSO_4$, both at 0.02 M concentration of copper.

The obtained filtrates were studied by X-ray Fluorescence (XRF) using a Bruker S8 Tiger dispersive wavelength X-ray spectrometer with 4 kW power, applying the Quant-Express method for light elements. A Rhodium tube was used as the X-ray source, and a high-precision goniometer was employed for theta and 2-theta angles to determine the concentrations of copper, sulfate, and chloride. The quantification of the copper nitrate solution was performed using ultraviolet-visible spectrophotometry with a Shimadzu UV-VIS spectrophotometer at a wavelength of 410 nm, following the protocol published by Jagessar and Sooknundun (2011).

Solid characterization

The X-ray diffraction (XRD) patterns of polycrystalline samples were measured using a Bruker D8 ADVANCE instrument with DA VINCI geometry, employing Cu $K\alpha_1$ radiation under the following conditions: 40 kV, 30 mA, Soller slits at 2.5° (Incidence and diffraction). The profile was measured from 3.5° to 70.0° 2θ with a step size of 0.015° 2θ, and samples were taken using continuous scanning. Morphological characterization was performed by Scanning Electron Microscopy (SEM) (FEI QUANTA 200). The 27Al NMR measurements were conducted with a Bruker Advance III-400 spectrometer, using a 4 mm solid-state probe and $Al(NO_3)_3$ as a reference at 0 ppm, with a central frequency of 78.14 MHz at ambient temperature. Finally, textural measurements were performed on a 3Flex Micromeritics instrument. The sample was degassed at 573 K for 8 hours, followed by nitrogen (N_2) adsorption/desorption at 75.062 K for 12 hours.

Results and discussion

X-ray diffraction patterns for the solid samples SOD1, SOD2, HDL2, and the composite SOD2-HDL2 are shown in Figure 1. Analysis of these patterns using the SEARCH/MATCH software and the ICDD PDF-4 database revealed that SOD1 exhibits a highly crystalline profile consistent with the sodalite-type phase, matching PDF card No. 76-1639. This indicates a well-formed synthetic zeolite structure with no detectable amorphous content.

Tecnología y Ciencias del Agua
OPEN ACCESS
Check for updates

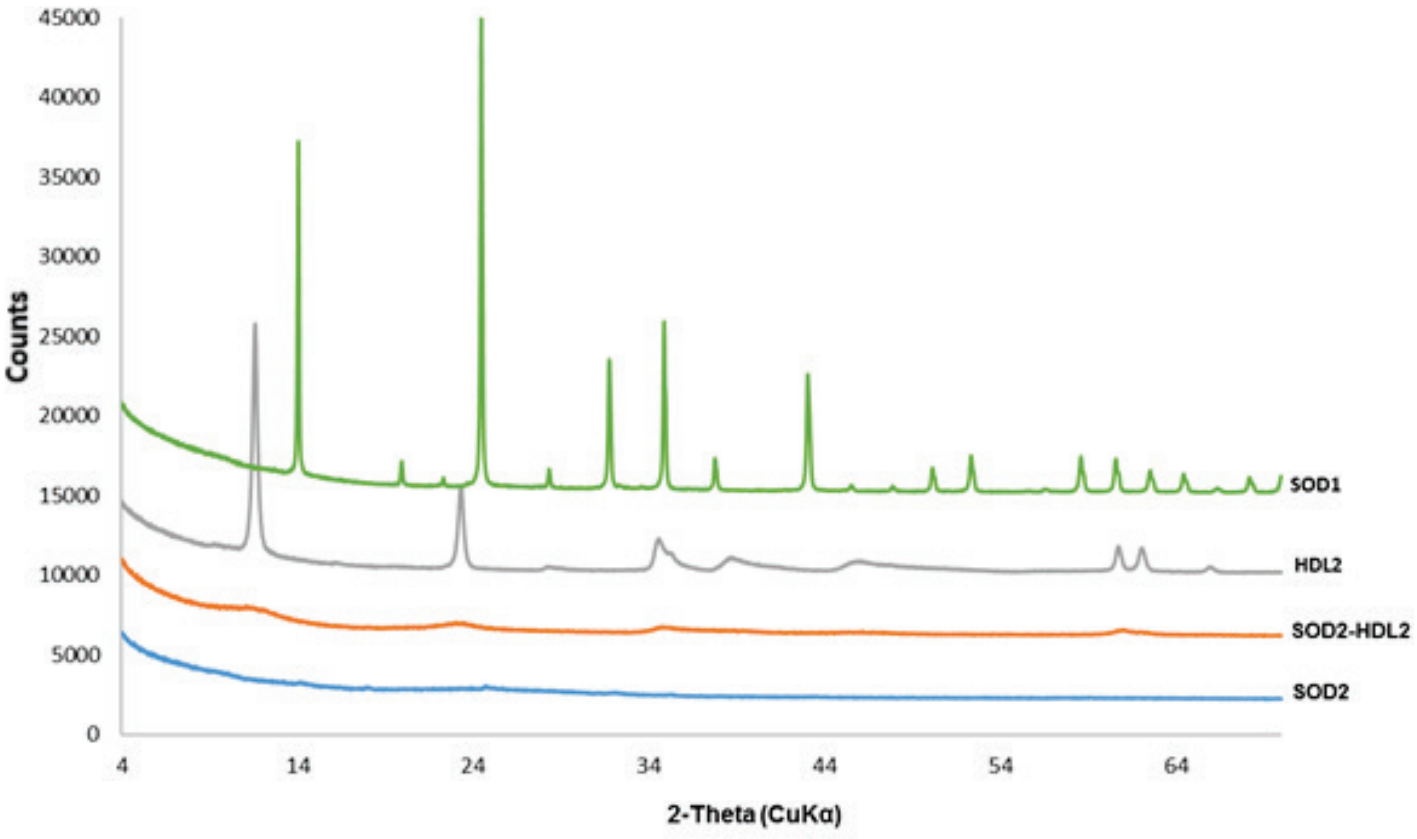

Figure 1. Diffraction profiles of the synthesized materials.

In the case of SOD2, the diffraction pattern confirms the retention of the same zeolitic phase; however, a notable decrease in crystallite size is evident. This is supported by the overall reduction in peak intensity (counts per second) across the diffractogram and a slight increase in background intensity around 25° 2θ. This behavior is attributed to the presence of $AlCl_3$, which acts as a Lewis acid and disrupts oxo-hydroxo bonds within the crystalline framework, leading to partial structural destabilization (Bernal & Railsback, 2008).

According to Figure 1, the HDL2 solid exhibits a crystalline diffraction pattern consistent with the PDF-35-965 reference phase. The

pattern indicates well-ordered lamellar stacking without turbostratic disorder, as evidenced by the symmetric reflection of the (003) plane located at 11.60° 2θ, showing no asymmetry (Forano, Hibino, Leroux, & Taviot-Guého, 2006). The diffractogram of the SOD2-HDL2 solid reveals the presence of HDL phases corresponding to PDF-43-72, while retaining the amorphous zeolite phase. This suggests the coexistence of both crystalline phases, with a possible coating of the sodalite-type zeolite crystallites by HDL nanosheets. This interpretation is further supported by SEM and NMR observations. Moreover, the absence of any shift in the (003) reflection, with the interlayer spacing remaining unchanged, implies that the anionic species between the layers are OH^- and CO_3^{2-}. In other words, no components from the zeolite were intercalated into the HDL structure, which is consistent with expectations for this material and in agreement with synthetic pathways reported for similar systems (Yamada *et al*., 2006; Wang *et al*., 2014; Yue *et al*., 2017; Zhang *et al*., 2019a, Zhang *et al*., 2019b).

Morphological analysis, shown in Figure 2, reveals the following: For the SOD1 solid, parallelepiped-shaped sodalite crystals ranging in size from 0.9 to 1.6 μm are observed, which tend to aggregate (Figure 2a). In the case of HDL2, the lamellar stacking characteristic of HDL crystals is evident, with various lamellar grains forming the crystalline structure (Figure 2b and 2c). Upon amorphization of the initial tectosilicate in SOD2, the crystal size decreases to 0.5–0.7 μm, while retaining the original morphology and aggregation behavior (Figure 2d). Finally, in the SOD2-HDL2 composite (Figure 2e), the presence of slightly distorted sodalite crystals is confirmed, along with an external coating by HDL layers. This observation closely resembles findings reported by Yamada *et al*. (2006) for LTA-type zeolite crystals. The formation of such a structure is

attributed to the basic character of the aluminosilicate surface, which promotes interactions with the residual positive charges associated with aluminum-centered octahedra in the HDL phase.

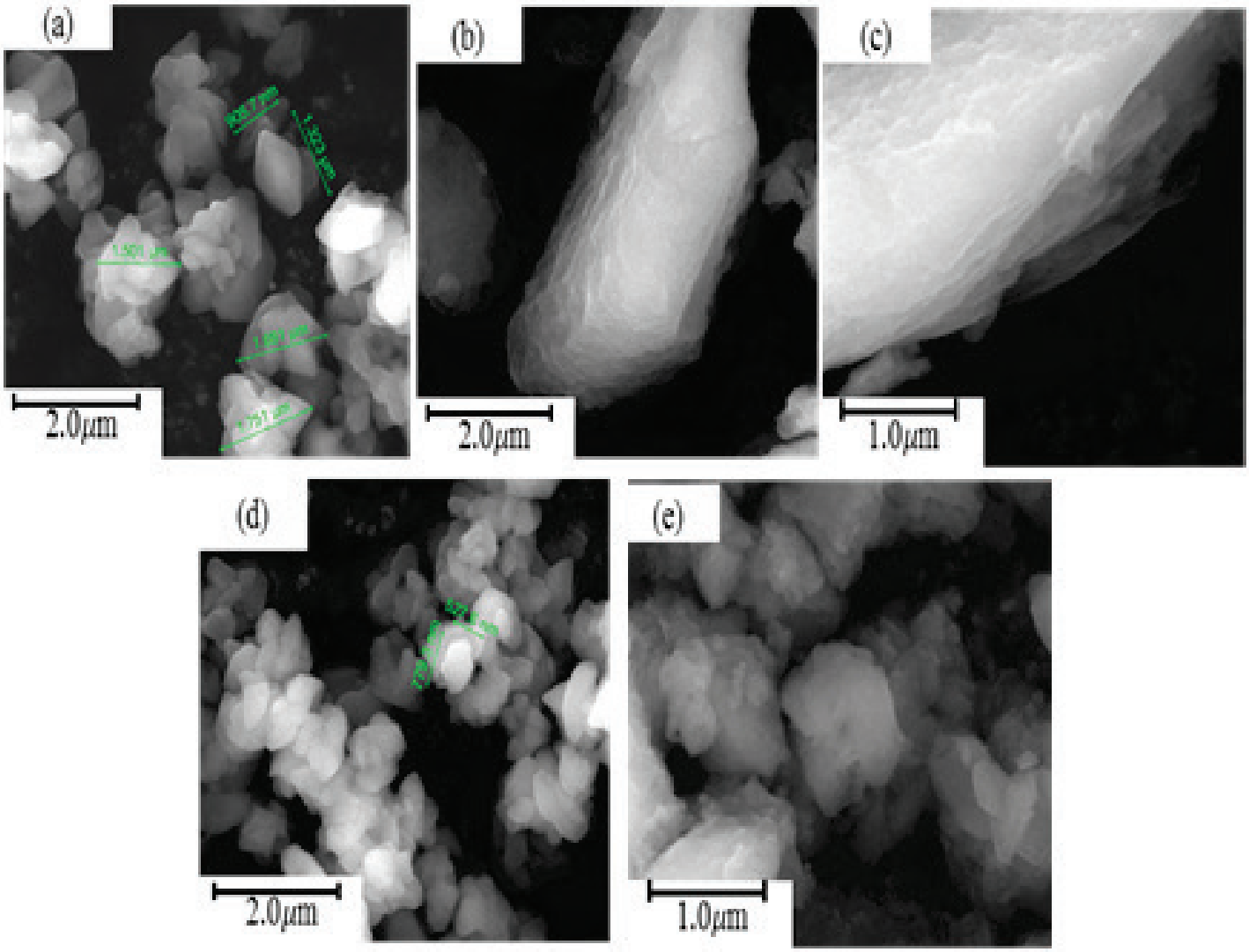

Figure 2. SEM images: (a) SOD1, (b) HDL2, (c) HDL2 — close-up of the lamellae, (d) SOD2, and (e) SOD2-HDL2.

The ^{27}Al MAS NMR spectra of the transition materials SOD1, HDL2, SOD2, and SOD2-HDL2 are shown in Figure 3 (a–d). A strong resonance around 50 ppm is observed for the SOD1 sample (Figure 3a) and with lower intensity for SOD2 (Figure 3c), indicating the presence of tetrahedral coordination in the sodalite zeolite structure before and after amorphization. These signals are characteristic of tectosilicate-type materials (Datt, Burns, Dhuna, & Larsen, 2013). The resonance near 0 ppm indicates the presence of octahedral coordination, as seen in the HDL2 (Figure 3b) and SOD2-HDL2 (Figure 3d) samples, corresponding to 6-coordinate aluminum in the HDL structure. This confirms the coexistence of both crystalline phases in the composite material.

Tecnología y Ciencias del Agua
OPEN ACCESS
Check for updates

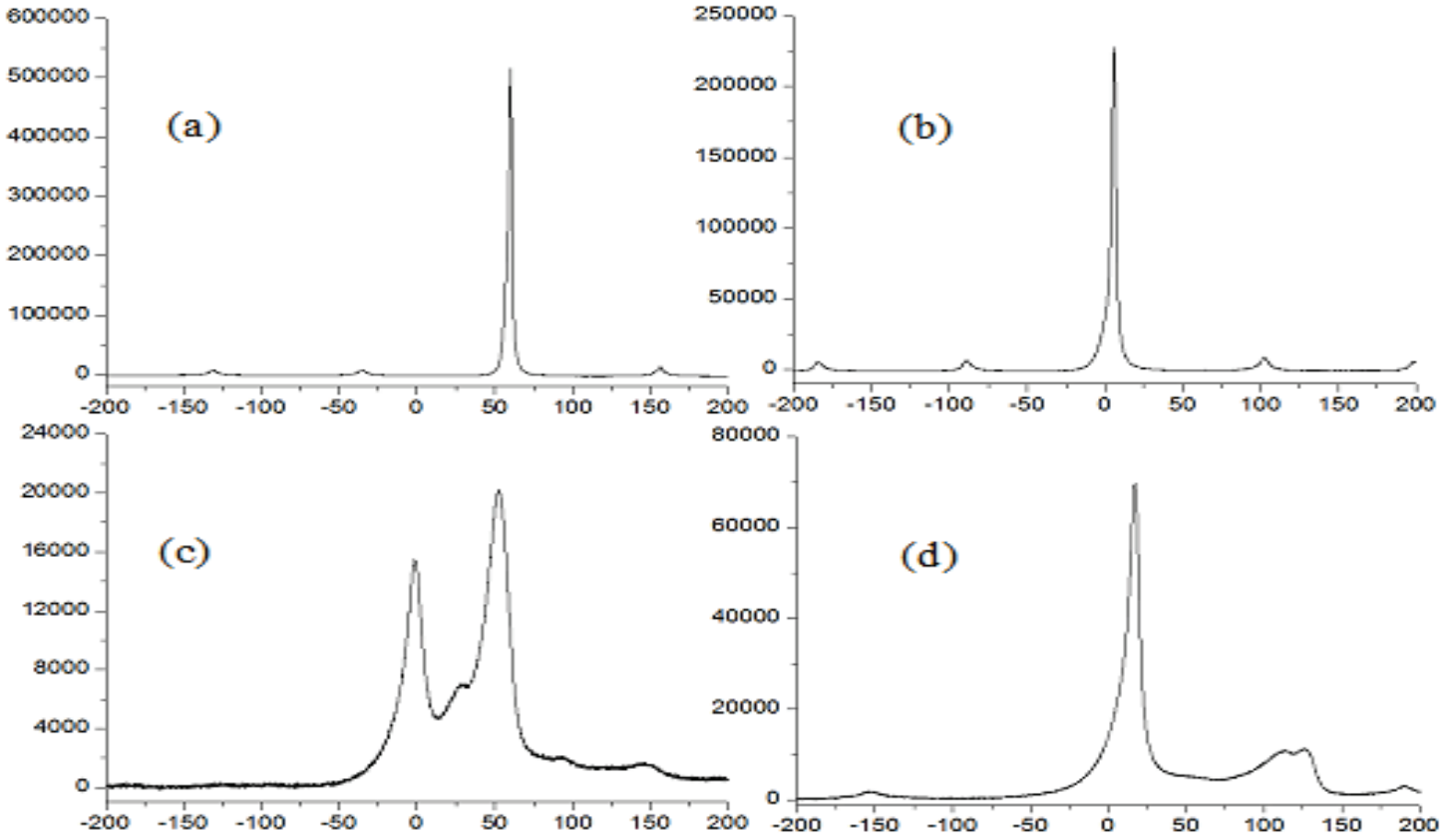

Figure 3. ^{27}Al MAS NMR spectra (v = 78.14 MHz) of the samples: (a) SOD1, (b) HDL2, (c) SOD2, and (d) SOD2-HDL2.

In Figure 3c, corresponding to the SOD2 sample, a splitting of the original signal is observed along with the appearance of new peaks attributed to hexacoordinate or extra-framework aluminum species around 0 ppm**.** The most intense resonance remains that of tetrahedrally coordinated aluminum at 50–60 ppm. Additional signals are observed at approximately 25 ppm, corresponding to pentacoordinate aluminum species, and in the 70–90 ppm range, attributed to free Al[45] species (Datt *et al*., 2013). The emergence of these new resonances, associated with

different aluminum coordination environments, indicates that the treatment with aluminum chloride disrupts the tetrahedral aluminum framework, generating various coordination geometries and particle sizes. This structural modification enhances the potential for interaction with copper salts on the material's surface.

In Figure 3d, corresponding to the SOD2-HDL2 sample, two distinct signals are observed in addition to the HDL2 signal at 0 ppm. A resonance at 60 ppm is attributed to tetrahedral aluminum in the zeolite framework, while a signal at 70 ppm corresponds to tetrahedrally coordinated aluminum in distorted HDL species (Di Bitetto, André, Carteret, Durand, & Kervern, 2017).

Figure 4 shows the N_2 adsorption/desorption isotherms, which reveal distinct behaviors for each sample. The HDL2 sample exhibits a type IV isotherm, characterized by a hysteresis loop associated with mesoporosity. This behavior results from capillary condensation, which limits adsorption at high relative pressures. These results suggest that the pH-controlled synthetic route promotes the formation of mesopores beyond those reported by Bezerra *et al*. (2019). In contrast, the SOD1 and SOD2 samples display type III isotherms, indicative of weak adsorbate–adsorbent interactions, typically associated with materials exhibiting low porosity or microporosity.

Tecnología y Ciencias del Agua

OPEN ACCESS

Check for updates

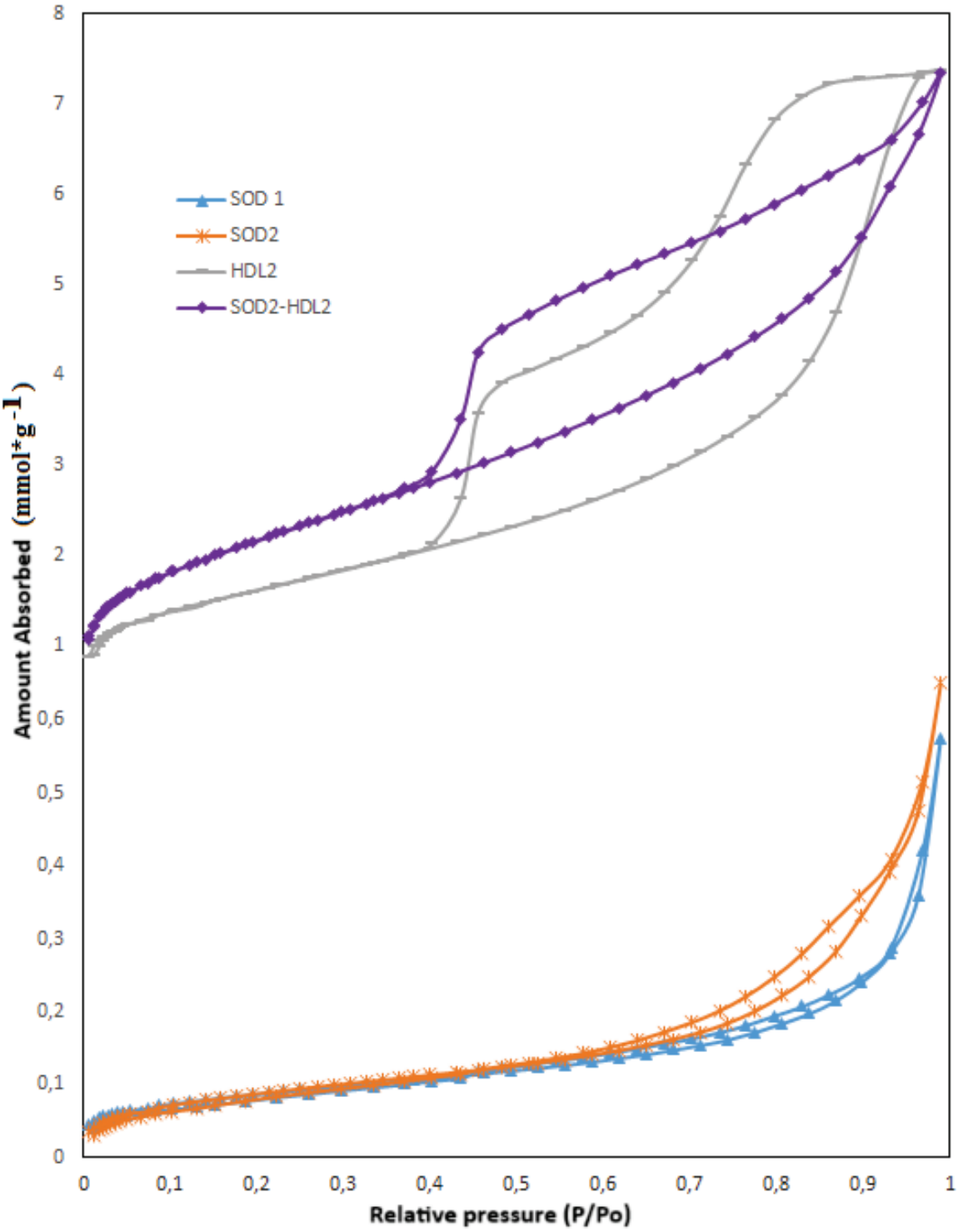

Figure 4. N_2 adsorption/desorption isotherms of the SOD1, SOD2, HDL2, and SOD2-HDL2 samples.

After synthesizing the materials to obtain the SOD2-HDL2 composite, it was observed that the adsorption/desorption curve is of type IV, with a shift from microporous to mesoporous character, associated with the characteristic hysteresis loop observed in such cases. These results are comparable to those obtained by Bezerra *et al*. (2019) for an LTA zeolite with an Mg/Al HDL ratio of 3. This leads to the conclusion that, in the case of sodalite, the coating of the materials increases their porosity

The analysis of the results obtained from the adsorption/desorption isotherms provided the BET surface area, pore volume, and average pore size values for the synthesized materials, which are presented in Table 1. The pore size values for all the materials fall within the range corresponding to mesoporous materials, which is 2–50 nm (Tian *et al*., 2025). The average pore size for HDL2 and SOD2 is considerably larger than that of the other materials, as shown in Table 1. This can be attributed to the fact that the pure crystalline phases maintain better crystal growth.

Table 1. Pore textural properties of SOD1, SOD2, HDL2, and SOD2-HDL2.

Sample	S_{BET} (m^2g^{-1})	V (cm^3g^{-1})	D(nm)
HDL2	127.99	0.242	7.57
SOD1	6.97	0.010	5.94
SOD2	7.25	0.014	8.07
SOD2-HDL2	175.33	0.219	5.00

The use of amorphizing agents such as $AlCl_3$ in the synthesis of the SOD2 solid, due to its nature as a Lewis acid, affects hydroxyl groups, leading to defects and alterations in the porous framework. This interaction promotes the displacement of sodium ions by extra-framework aluminum, which in turn increases the size of hydration spheres and results in enlarged pore diameters. The SOD2-HDL2 sample exhibits a smaller average pore size, which may be attributed to the tertiary structure of sodalite containing microporous nuclei that can interact with similarly structured nuclei within the HDL phase. This interaction likely leads to more extensive coverage of the HDL grains, thereby reducing the apparent pore accessibility (Contini, Jendrlin, Al-Ani, & Zholobenko, 2024).

The coated materials exhibit greater pore volume and pore size compared to LTA-type zeolites synthesized with varying amounts of organosilanes used as surfactants (Lucena *et al*., 2022). The materials synthesized in this study also show higher specific surface area and pore volume than LTA zeolites, HDL with a Mg/Al ratio of 3, and the coated materials reported by Bezerra *et al*. (2016), highlighting progress in the development of materials with potential applications in removal processes and catalysis.

The BET surface area increases after coating the HDL with SOD2 zeolite, despite the relatively low surface area of pure SOD2 compared to sodalite-type zeolites reported by Derkowski, Franus, Beran and Czímerová (2006). This enhancement is even more pronounced when the HDL is deposited onto aluminosilicate crystals. The resulting increase in surface area significantly improves the material's interaction with potential substrates in catalytic processes.

As shown in Table 2, after mixing the four previously characterized materials with 0.02 M solutions of copper nitrate, sulfate, and chloride, all materials exhibited Cu^{2+} ion uptake, ranging from 2.31 to 9.26 mmol Cu^{2+} per gram of material. For the sodalite zeolite (SOD1), the copper ion removal capacity from nitrate solution is comparable to that reported by Quintana *et al*. (2014), confirming that the sodalite-type cavity in both structures is responsible for accommodating the Cu^{2+} cation.

Table 2. Percentage of Cu^{2+}, NO_3^-, SO_4^{2-} and Cl^- ions fixed in the solids.

Sample	Copper nitrate		Copper sulfate		Copper chloride	
	*Cu^{2+}	* NO_3^-	* Cu^{2+}	* SO_4^{2-}	* Cu^{2+}	* Cl^-
SOD1	4.84 ±0.02	12.20 ±0.02	5.41 ±0.01	0.00	5.83 ±0.01	4.17 ±0.01
SOD2	2.31 ±0.01	13.21 ±0.01	4.88 ±0.02	3.20 ±0.01	2.35 ±0.01	3.60 ±0.01
LDH2	4.30 ±0.01	13.50 ±0.02	6.06 ±0.02	4.59 ±0.02	4.31 ±0.01	4.69 ±0.01
SOD2-LDH2	**7.28 ±0.02**	**14.41 ±0.02**	**9.10 ±0.01**	**8.82 ±0.02**	**9.26 ±0.02**	**9.34 ±0.02**

The variation in Cu^{2+} removal efficiency is attributed to the influence of the accompanying anion, as it has been demonstrated that the anion significantly affects the cation's removal from the target solution. For SOD1 and SOD2-HDL2, which are more basic materials than amorphized sodalite and HDL, the removal follows the trend $Cl^- > SO_4^{2-} > NO_3^-$. In contrast, for the less basic amorphized sodalite and HDL, copper removal is highest when derived from SO_4^{2-}, followed by Cl^- and then NO_3^-. This

behavior can be explained by differences in anion polarizability, which in turn influence the size of hydration spheres (Bergström, Lindgren, & Kristiansson, 1991).

These findings indicate that the synthesized materials exhibit superior Cu^{2+} removal capacities compared to DOWEX 50W resins (4.6 $mmol \cdot g^{-1}$) (Pehlivan & Altun, 2006), layered double hydroxide (LDH) with Mg/Al = 3 (0.37 $mmol \cdot g^{-1}$), and other systems such as mercaptoethane sulfate nanoparticles (Bezerra *et al*., 2019; Vicente-Martínez, Caravaca-Garratón, García-Onsurbe, & Soto-Meca, 2021), treated biomass like tuber peels, and marine species-based biosorbents (Aman, Kazi, Sabri, & Bano, 2008; Panfili, Bartucca, Ballerini, & Del Buono, 2017).

In terms of anion removal, the synthesized sodalite and HDL materials demonstrated sulfate, nitrate, and chloride retention capabilities—except for SOD1, which showed no sulfate uptake. This lack of removal may be due to the larger hydration sphere of sulfate compared to the pore size of the zeolite (Bergström *et al*., 1991). The overall anion removal capacity surpasses that reported for natural LTA-type zeolites and LDH with Mg/Al = 3, either individually or as composites (Yuan *et al*., 2018; Bezerra *et al*., 2019; Zhang *et al*., 2019b) highlighting the higher surface basicity of the materials developed in this work.

Furthermore, the results demonstrate that coating a basic tectosilicate with an HDL of low Mg/Al molar ratio significantly enhances the material's ability to retain both anions and cations. This behavior contrasts with that observed in systems involving less basic LTA zeolites and HDL with higher Mg/Al ratios, where reduced retention is observed. This inverse trend may be associated with the precipitation of copper hydroxy salts and their counter-anions within the internal structure and

on the surfaces of the crystalline frameworks and layered sheets (Bezerra *et al*., 2019).

In addition, the removal capacities for both cations and anions from contaminated salts—measured in moles per gram of coated material—are notably higher than those reported for chlorine-based HDL (2.01 mmol Cr^{6+}/g) (Yue *et al*., 2017), hydrotalcite (0.58 mmol Cr^{6+}/g) (Wang *et al*., 2014), Mg-Fe^{3+} HDL (0.11 mmol Cr^{6+}/g) (García-Sosa *et al*., 2015), modified zeolites (0.02 mmol Cr^{6+}/g) (Salgado-Gómez, Macedo-Miranda, & Olguín, 2014), and synthetic phillipsite-type zeolites used for the inclusion of ions such as rhodium, calcium, and copper (López *et al*., 2020).

Conclusions

A synthetic route was successfully developed for obtaining sodalite-type zeolite, hydrotalcite-like layered double hydroxide (HDL), and an HDL-coated tectosilicate using post-consumer materials. The resulting materials demonstrate that parallelepiped-shaped sodalite grains are coated with HDL nanosheets containing both octahedral and tetrahedral aluminum coordination, with minor structural distortions. The materials exhibit Type IV isotherms, a significantly higher specific surface area than typical sodalite, mesoporosity, and high ion exchange capacity. The HDL-coated sodalite-based material showed effective removal capacities for Cu^{2+} cations and Cl^-, NO_3^-, and SO_4^{2-} anions, reaching up to 9.26 $mmol \cdot g^{-1}$ for Cu^{2+}, and 9.34 $mmol \cdot g^{-1}$, 8.82 $mmol \cdot g^{-1}$, and 14.41 $mmol \cdot g^{-1}$ for Cl^-, SO_4^{2-}, and NO_3^-, respectively. These results highlight the potential of the synthesized materials for applications in water remediation and ion exchange processes.

References

Aman, T., Kazi, A. A., Sabri, M. U., & Bano, Q. (2008). Potato peels as solid waste for the removal of heavy metal copper (II) from waste water/industrial effluent. *Colloids and Surfaces B: Biointerfaces*, 63(1), 116-121. DOI: https://doi.org/10.1016/j.colsurfb.2007.11.013

Bergström, P. A., Lindgren, J., & Kristiansson, O. (1991). An IR study of the hydration of perchlorate, nitrate, iodide, bromide, chloride and sulfate anions in aqueous solution. *The Journal of Physical Chemistry*, 95(22), 8575-8580. DOI: https://doi.org/10.1021/j100175a031

Bernal, J. P., & Railsback, L. B. (2008). Introducción a la tabla periódica de los elementos y sus iones para ciencias de la tierra. *Revista Mexicana de Ciencias Geológicas*, 25(2), 236-246.

Bezerra, B. G. P., Bieseki, L., Da Silva, D. R., & Pergher, S. B. C. (2019). Development of a zeolite A/LDH composite for simultaneous cation and anion removal. *Materials*, 12(4), 661. DOI: https://doi.org/10.3390/ma12040661

Cataldo, E., Salvi, L., Paoli, F., Fucile, M., Masciandaro, G., Manzi, D., Masini, C. M., & Mattii, G. B. (2021). Application of zeolites in agriculture and other potential uses: A review. *Agronomy*, 11(8), 1547. DOI: https://doi.org/10.3390/agronomy11081547

Chung, J., Lee, J., Kim, J. K., Kim, M., Lee, K. S., Kim, S. J., Lee, M. H., & Yu, T. (2020). An analytical method to characterize the crystal structure of layered double hydroxides: Synthesis, characterization, and electrochemical studies of zinc-based LDH nanoplates. *Journal of Materials Chemistry A*, 8(17), 8692-8699. DOI: https://doi.org/10.1039/D0TA01774D

Contini, A., Jendrlin, M., Al-Ani, A., & Zholobenko, V. (2024). Structural and acidic properties of ion-exchanged mazzite. *Petroleum Chemistry*, 64(3), 1-10. DOI: https://doi.org/10.1134/S0965544123110099

Datt, A., Burns, E. A., Dhuna, N. A., & Larsen, S. C. (2013). Loading and release of 5-fluorouracil from HY zeolites with varying SiO_2 /Al_2 O_3 ratios. *Microporous and Mesoporous Materials*, 167, 182-187. DOI: https://doi.org/10.1016/j.micromeso.2012.09.011

Derkowski, A., Franus, W., Beran, E., & Czímerová, A. (2006). Properties and potential applications of zeolitic materials produced from fly ash using simple method of synthesis. *Powder Technology*, 166(1), 47-54. DOI: https://doi.org/10.1016/j.powtec.2006.05.004

Di Bitetto, A., André, E., Carteret, C., Durand, P., & Kervern, G. (2017). Probing the dynamics of layered double hydroxides by solid-state ^{27}Al NMR spectroscopy. *The Journal of Physical Chemistry C*, 121(13), 7276-7281. DOI: https://doi.org/10.1021/acs.jpcc.6b13106

Forano, C., Hibino, T., Leroux, F., & Taviot-Guého, C. (2006). Layered double hydroxides. *Developments in Clay Science*, 1, 1021-1095. DOI: https://doi.org/10.1016/S1572-4352(05)01039-1

García-Sosa, I., Cabral-Prieto, A., Nava, N., Navarrete, J., Olguín, M. T., Escobar, L., López-Castañares, R., & Olea-Cardoso, O. (2015). Sorption of chromium (VI) by Mg/Fe hydrotalcite-type compounds. *Hyperfine Interactions*, 232, 67-75. DOI: https://doi.org/10.1007/s10751-014-1117-5

Guilherme, V. A., Cunha, V. R., De Paula, E., De Araujo, D. R., & Constantino, V. R. (2022). Anti-inflammatory and analgesic evaluation of a phytochemical intercalated into layered double hydroxide. *Pharmaceutics*, 14(5), 934. DOI: https://doi.org/10.3390/pharmaceutics14050934

Hong, S. J., Ryu, J. Y., Lee, J. Y., Kim, C., Kim, S. J., & Kim, Y. (2004). Synthesis, structure and heterogeneous catalytic activities of Cu-containing polymeric compounds: Anion effect and comparison of homogeneous vs. heterogeneous catalytic activity. *Dalton Transactions*, 17, 2697-2701. DOI: https://doi.org/10.1039/B406877G

Jagessar, R. C., & Sooknundun, L. (2011). Determination of nitrate anion in waste water from nine selected areas of coastal Guyana via a spectrophotometric method. *International Journal of Research and Reviews in Applied Sciences*, 7(2), 203-212.

Ji, Y., Zhang, X., Gao, J., Zhao, S., Dou, Y., Xue, Y., & Chen, L. (2020). Efficiency and mechanisms of cadmium removal via core-shell zeolite/Zn-layer double hydroxides. *Ecotoxicology and Environmental Safety*, 188, 109887. DOI: https://doi.org/10.1016/j.ecoenv.2019.109887

Kumari, S., Sharma, V., Soni, S., Sharma, A., Thakur, A., Kumar, S., Dhama, K., Sharma, A. K., & Bhatia, S. K. (2023). Layered double hydroxides and their tailored hybrids/composites: Progressive trends for delivery of natural/synthetic-drug/cosmetic biomolecules. *Environmental Research*, 231, 117171. DOI: https://doi.org/10.1016/j.envres.2023.117171

Lee, H., Wu, X., & Sun, L. (2020). Copper-based homogeneous and heterogeneous catalysts for electrochemical water oxidation. *Nanoscale*, 12(7), 4187-4218. DOI: https://doi.org/10.1039/C9NR10437B

Li, H., Li, S., Guan, R., Jin, Z., Xiao, D., Guo, Y., & Li, P. (2024). Modulating the surface concentration and lifetime of active hydrogen in Cu-based layered double hydroxides for electrocatalytic nitrate reduction to ammonia. *ACS Catalysis*, 14(16), 12042-12050. DOI: https://doi.org/10.1021/acscatal.4c03245

Liu, S., Lian, X., Yue, B., Xu, S., Wu, G., Chai, Y., Zhang, Y., & Li, L. (2024). Control of zeolite local polarity toward efficient xenon/krypton separation. *Journal of the American Chemical Society*, 146(12), 8335-8342. DOI: https://doi.org/10.1021/jacs.3c13994

López, J. A., Toro, R. A., Romero-Bohórquez, A. R., Quintana, J. H., & Henao, J. A. (2020). Synthesis of zeolites P and evaluation of their activity as new and reusable heterogeneous catalysts in a three-component ABB'Povarov model reaction. *Universitas Scientiarum*, 25(3), 385-407. DOI: https://doi.org/10.11144/Javeriana.SC25-3.sozp

Lucena, S. M., De Oliveira, J. C. A., Vasconcelos-Gonçalves, D. V., Lucas, L. M., Moura, P. A., Gomes-Santiago, R. G., Azevedo, D., & Bastos-Neto, M. (2022). LTA zeolite characterization based on pore type distribution. *Industrial & Engineering Chemistry Research*, 61(5), 2268-2279. DOI: https://doi.org/10.1021/acs.iecr.1c04897

Panfili, I., Bartucca, M. L., Ballerini, E., & Del Buono, D. (2017). Combination of aquatic species and safeners improves the remediation of copper polluted water. *Science of the Total Environment*, 601, 1263-1270. DOI: https://doi.org/10.1016/j.scitotenv.2017.06.003

Pehlivan, E., & Altun, T. (2006). The study of various parameters affecting the ion exchange of Cu^{2+}, Zn^{2+}, Ni^{2+}, Cd^{2+}, and Pb^{2+} from aqueous solution on Dowex 50W synthetic resin. *Journal of Hazardous Materials*, 134(1-3), 149-156. DOI: https://doi.org/10.1016/j.jhazmat.2005.10.052

Quintana, J. H., Aparicio, A. P., Parra, L. K., Henao, J. A., & Ríos, C. A. (2014). Estudio de parámetros de síntesis de las estructuras zeolíticas Linde Tipo A (LTA) y Faujasita (FAU) X a partir de aluminio post-consumo y diatomita, para la remoción de metales pesados. *Revista de la Academia Colombiana de Ciencias Exactas, Físicas y Naturales*, 38(148), 167-180. DOI: https://doi.org/10.18257/raccefyn.162

Salgado-Gómez, N., Macedo-Miranda, M. G., & Olguín, M. T. (2014). Chromium VI adsorption from sodium chromate and potassium dichromate aqueous systems by hexadecyltrimethylammonium-modified zeolite-rich tuff. *Applied Clay Science*, 95, 197-204. DOI: https://doi.org/10.1016/j.clay.2014.04.013

Szerement, J., Szatanik-Kloc, A., Jarosz, R., Bajda, T., & Mierzwa-Hersztek, M. (2021). Contemporary applications of natural and synthetic zeolites from fly ash in agriculture and environmental protection. *Journal of Cleaner Production*, 311, 127461. DOI: https://doi.org/10.1016/j.jclepro.2021.127461

Teixeira, S. C. G., Mathias, L., & Canela, M. C. (2003). Recuperação de sílica-gel utilizando processos oxidativos avançados: Uma alternativa simples e de baixo custo. *Química Nova*, 26(6), 931-933. DOI: https://doi.org/10.1590/S0100-40422003000600025

Theiss, F. L., Couperthwaite, S. J., Ayoko, G. A., & Frost, R. L. (2014). A review of the removal of anions and oxyanions of the halogen elements from aqueous solution by layered double hydroxides. *Journal of Colloid and Interface Science*, 417, 356-368. DOI: https://doi.org/10.1016/j.jcis.2013.11.040

Tian, K., Tan, D., Fu, X., Zhang, Y., Yao, D., Zhong, M., Chen, R., Dong, Y., & Liu, Y. (2025). Adsorption performance of 1,4-dioxane by MCM-22 and Beta zeolites and their bio-zeolite composite system in the presence of co-contaminants. *Separation and Purification Technology*, 354, 128752. DOI: https://doi.org/10.1016/j.seppur.2024.128752

Vicente-Martínez, Y., Caravaca-Garratón, M., García-Onsurbe, M. D. C., & Soto-Meca, A. (2021). Silver nanoparticles functionalized with sodium mercaptoethane sulfonate to remove copper from water by the formation of a micellar phase. *Separations*, 8(8), 108. DOI: https://doi.org/10.3390/separations8080108

Wang, W., Zhou, J., Achari, G., Yu, J., & Cai, W. (2014). Cr(VI) removal from aqueous solutions by hydrothermal synthetic layered double hydroxides: Adsorption performance, coexisting anions and regeneration studies. *Colloids and Surfaces A: Physicochemical and Engineering Aspects*, 457, 33-40. DOI: https://doi.org/10.1016/j.colsurfa.2014.05.034

Weitkamp, J. (2000). Zeolites and catalysis. *Solid State Ionics*, 131(1-2), 175-188. DOI: https://doi.org/10.1016/S0167-2738(00)00632-9

Xie, Z. H., Zhou, H. Y., He, C. S., Pan, Z. C., Yao, G., & Lai, B. (2021). Synthesis, application and catalytic performance of layered double hydroxide based catalysts in advanced oxidation processes for wastewater decontamination: A review. *Chemical Engineering Journal*, 414, 128713. DOI: https://doi.org/10.1016/j.cej.2021.128713

Yamada, H., Watanabe, Y., Hashimoto, T., Tamura, K., Ikoma, T., Yokoyama, S., Tanaka, J., & Moriyoshi, Y. (2006). Synthesis and characterization of Linde A zeolite coated with a layered double hydroxide. *Journal of the European Ceramic Society*, 26(4-5), 463-467. DOI: https://doi.org/10.1016/j.jeurceramsoc.2005.07.018

Yang, Z. Z., Zhang, C., Zeng, G. M., Tan, X. F., Huang, D. L., Zhou, J. W., Fang, Q.-Z., Yang, K.-H., Wang H., Wei, J., & Nie, K. (2021). State-of-the-art progress in the rational design of layered double hydroxide based photocatalysts for photocatalytic and photoelectrochemical H_2 /O_2 production. *Coordination Chemistry Reviews*, 446, 214103. DOI: https://doi.org/10.1016/j.ccr.2021.214103

Yuan, E. H., Han, R., Deng, J. Y., Zhou, W., & Zhou, A. (2024). Acceleration of zeolite crystallization: Current status, mechanisms, and perspectives. *ACS Applied Materials & Interfaces*, 16(23), 29521-29546. DOI: https://doi.org/10.1021/acsami.4c01774

Yuan, Y., Zhang, X., Lei, Y., Jiang, Y., Xu, Z., Zhang, S., Gao, J., & Zhao, S. (2018). Nitrogen removal by modified zeolites coated with Zn-layered double hydroxides (Zn-LDHs) prepared at different molar ratios. *Journal of the Taiwan Institute of Chemical Engineers*, 87, 73-82. DOI: https://doi.org/10.1016/j.jtice.2018.03.010

Yue, X., Liu, W., Chen, Z., & Lin, Z. (2017). Simultaneous removal of Cu(II) and Cr(VI) by Mg-Al-Cl layered double hydroxide and mechanism insight. *Journal of Environmental Sciences*, 53, 16-26. DOI: https://doi.org/10.1016/j.jes.2016.01.015

Zhang, Q., Li, J., Wang, X., He, G., Li, L., Xu, J., Mei, D., Terasaki, O., & Yu, J. (2023). Silanol-engineered nonclassical growth of zeolite nanosheets from oriented attachment of amorphous protozeolite nanoparticles. *Journal of the American Chemical Society*, 145(39), 21231-21241. DOI: https://doi.org/10.1021/jacs.3c04031

Zhang, X., Gao, J., Lei, Y., Xu, Z., Xia, S., Jiang, Y., & Cheng, J. (2019a). Phosphorus removal and mechanisms by Zn-layered double hydroxide (Zn-LDHs)-modified zeolite substrates in a constructed rapid infiltration system. *RSC Advances*, 9(68), 39811-39823. DOI: https://doi.org/10.1039/C9RA04826J

Zhang, X., Gao, J., Zhao, S., Lei, Y., Yuan, Y., He, C., Gao, C., & Deng, L. (2019b). Hexavalent chromium removal from aqueous solution by adsorption on modified zeolites coated with Mg-layered double hydroxides. *Environmental Science and Pollution Research*, 26, 32928-32941. DOI: https://doi.org/10.1007/s11356-019-06410-5